Research Article

Effect of electroacupuncture on glial fibrillary acidic protein and nerve growth factor in the hippocampus of rats with hyperlipidemia and middle cerebral artery thrombus

https://doi.org/10.4103/1673-5374.286973

Received: November 2, 2019

Peer review started: December 2, 2019

Accepted: January 19, 2020

Published online: August 10, 2020

Na-Ying Xue[1], Dong-Yu Ge[2], Rui-Juan Dong[2], Hyung-Hwan Kim[3], Xiu-Jun Ren[1,*], Ya Tu[1,*]

Graphical Abstract *Effect of electroacupuncture (EA) on hyperlipidemia and middle artery thrombus*

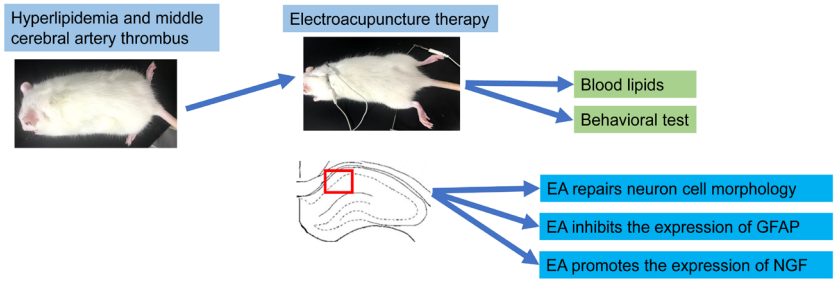

Abstract

Electroacupuncture (EA) has been shown to reduce blood lipid level and improve cerebral ischemia in rats with hyperlipemia complicated by cerebral ischemia. However, there are few studies on the results and mechanism of the effect of EA in reducing blood lipid level or promoting neural repair after stroke in hyperlipidemic subjects. In this study, EA was applied to a rat model of hyperlipidemia and middle cerebral artery thrombosis and the condition of neurons and astrocytes after hippocampal injury was assessed. Except for the normal group, rats in other groups were fed a high-fat diet throughout the whole experiment. Hyperlipidemia models were established in rats fed a high-fat diet for 6 weeks. Middle cerebral artery thrombus models were induced by pasting 50% $FeCl_3$ filter paper on the left middle cerebral artery for 20 minutes on day 50 as the model group. EA1 group rats received EA at bilateral ST40 (*Fenglong*) for 7 days before the thrombosis. Rats in the EA1 and EA2 groups received EA at GV20 (*Baihui*) and bilateral ST40 for 14 days after model establishment. Neuronal health was assessed by hematoxylin-eosin staining in the brain. Hyperlipidemia was assessed by biochemical methods that measured total cholesterol, triglyceride, low-density lipoprotein and high-density lipoprotein in blood sera. Behavioral analysis was used to confirm the establishment of the model. Immunohistochemical methods were used to detect the expression of glial fibrillary acidic protein and nerve growth factor in the hippocampal CA1 region. The results demonstrated that, compared with the model group, blood lipid levels significantly decreased, glial fibrillary acidic protein immunoreactivity was significantly weakened and nerve growth factor immunoreactivity was significantly enhanced in the EA1 and EA2 groups. The repair effect was superior in the EA1 group than in the EA2 group. These findings confirm that EA can reduce blood lipid, inhibit glial fibrillary acidic protein expression and promote nerve growth factor expression in the hippocampal CA1 region after hyperlipidemia and middle cerebral artery thrombosis. All experimental procedures and protocols were approved by the Animal Use and Management Committee of Beijing University of Chinese Medicine, China (approval No. BUCM-3-2018022802-1002) on April 12, 2018.
Key Words: astrocytes; CA1; cerebral ischemia; electroacupuncture; glial fibrillary acidic protein; hematoxylin-eosin staining; hippocampus; hyperlipidemia; immunohistochemistry; nerve growth factor

Chinese Library Classification No. R459.9; R363; R364

Introduction

According to the data from the 2018 China Health Statistics Summary (Wang et al., 2019), cerebrovascular diseases accounted for more than 20.52% of deaths among Chinese residents in 2017. Hyperlipidemia is strongly associated with cerebrovascular diseases, such as atherosclerosis and stroke (Yang et al., 2018). Previous studies have shown that long-term elevated cholesterol level activates pathological processes, including oxidative stress, endothelial dysfunction, blood-brain barrier dysfunction and intravascular thrombosis

[1]School of Acupuncture-Moxibustion and Tuina, Beijing University of Chinese Medicine, Beijing, China; [2]School of Traditional Chinese Medicine, Beijing University of Chinese Medicine, Beijing, China; [3]Neurovascular Research Laboratory, Department of Radiology, Massachusetts General Hospital and Harvard Medical School, Charlestown, MA, USA

*Correspondence to: Xiu-Jun Ren, MD, PhD, rxiujun@163.com; Ya Tu, MD, PhD, tuyab@263.net.

https://orcid.org/0000-0002-4912-0420 (Xiu-Jun Ren); https://orcid.org/0000-0002-6777-2588 (Ya Tu)

Funding: *This study was funded by the National Natural Science Foundation of China, No. 81470200 (to XJR).*

How to cite this article: *Xue NY, Ge DY, Dong RJ, Kim HH, Ren XJ, Tu Y (2021) Effect of electroacupuncture on glial fibrillary acidic protein and nerve growth factor in the hippocampus of rats with hyperlipidemia and middle cerebral artery thrombus. Neural Regen Res 16(1):137-142.*

(Cao et al., 2015), that exacerbate cerebral ischemia injury and thus increase stroke mortality. Therefore, normalizing blood lipid levels is of great clinical significance for the treatment and prognosis of stroke. Astrocytes play key roles in the brain, including regulating neuronal activity, supporting synaptic plasticity and neurogenesis. They are now considered important targets for manipulating delays in neuronal damage after focal cerebral ischemia and global cerebral ischemia (Ouyang et al., 2014). Nerve growth factor (NGF) is a prototypical target-derived neurotrophic factor (O'Keeffe et al., 2016). Pyramidal neurons in hippocampal CA1 region of rats are particularly vulnerable to ischemic injury (Li et al., 2019). The relationship between astrocytes and NGF in the repair of neurons in the hippocampus was explored in this study. Thrombolysis is the only Food and Drug Administration-approved method for the treatment of acute stroke, but it is risky, has a limited treatment time window and has few benefits (Han et al., 2013).

Electroacupuncture (EA) on GV20 (*Baihui*) and ST40 (*Fenglong*) is the method in traditional Chinese Medicine for preventing and treating ischemic stroke proposed by Professor Ya Tu according to clinical symptoms and compatibility. It can promote blood circulation by removing blood stasis. Because patients with hyperlipidemia are often more susceptible to stroke, this study used a rat model of hyperlipidemia and middle cerebral artery thrombus (hMCAT), which was induced by 50% $FeCl_3$. The rat model is relatively close to human clinical manifestations. Previous work showed that the model is simple and stable (Mao et al., 2018). The death and disability rate are low. Rats exhibited a high blood lipid serum level after eating a high-fat diet for 6 weeks, and then suffered severe neurological deficits after cerebral ischemia.

This study was designed to observe the effect of EA on the condition of neuronal cells and the changes of glial fibrillary acidic protein (GFAP) and NGF in the hippocampus by EA intervention in hMCAT model rats.

Materials and Methods

Animals

All experimental procedures and protocols were approved by the Animal Use and Management Committee of Beijing University of Chinese Medicine (approval No. BUCM-3-2018022802-1002) on April 12, 2018. This study was conducted in line with the NIH Guide for the Care and Use of Laboratory Animals (National Reseacher Conucil, 2011).

Fifty-seven male 7-week specific-pathogen-free Sprague-Dawley rats, weighing 180–220 g, were provided by Beijing Vital River Laboratory Animal Technology Co., Ltd., Beijing, China (license No. SCXK (Jing) 2012-0001). Three died from surgical complications. The rats were raised in specific-pathogen-free laboratory of Beijing University of Chinese Medicine, China. They were housed in plastic cages (5 rats per cage) with wood-shaving bedding at room temperature of 23 ± 2°C and humidity of 55 ± 5%. The cages were well ventilated and cleaned regularly. Rats were kept under illumination from 07:00 to 19:00 daily, with free access to filtered water and feed.

Groups

Fifty-seven rats were randomly divided into normal control (normal, n = 5), sham (sham operation, n = 11), model (n = 13), EA1 group (n = 14) and EA2 group (n = 14). Rats in the normal group were fed with ordinary diet for 63 days and had no operations. Rats in all other groups were fed the high-fat diet for 63 days. The sham group had their middle cerebral artery exposed on day 50 but no MCAT was established. Rats in the model group had MCAT induced on day 50 but did not receive EA. Rats in the EA1 group received EA, 20 minutes daily, at bilateral ST40 from day 43 to 49 then MCAT models were established on day 50. The EA1 rats also received EA at GV20 and bilateral ST40 from day 50 to 63. The EA2 group had MCAT models established on day 50. The EA2 rats received EA at GV20 and bilateral ST40 daily from day 50 to 63 (**Figure 1**).

Animal model establishment

Hyperlipidemia models

According to a previous study, rats were fed with a classic high-fat diet for 6 weeks to create hyperlipidemia models (Baldivia et al., 2018). The formula is 1% cholesterol, 10% egg yolk powder, 5% lard, 0.5% sodium cholate and 83.5% standard forage (Beijing Keao Xieli feed Co., Ltd., Beijing, China). This study fed the diet for six weeks before the first EA treatment in the EA1 group and continued for a further week in all experimental groups until operated on. Rats were selected (after 6 weeks of diet) when their serum total cholesterol (TC) had increased significantly compared with that in the normal group (P < 0.05).

Middle cerebral artery thrombosis (MCAT) models

Rats were intraperitoneally anesthetized with 10% sodium pentobarbital (40 mg/kg) and laid in the right lateral decubitus position. A 2 cm longitudinal incision in the skin was cut at the mid-point between the back of the left orbit and the ear. The left temporal muscle was removed to expose the temporal bone. A bone window with a diameter of 5 mm was made by a high-speed dental drill (Strong 90, Saeshin Precision Co., Ltd., Daegu, South Korea). After lifting the skull with forceps, the trace of the middle cerebral artery was visualized. A 2 × 2 mm^2 filter paper, soaked in 50% $FeCl_3$ (Tianjin Fuchen Chemical Reagents Factory, Tianjin, China) in 0.1 M HCL, was applied to the left middle cerebral artery for 20 minutes. After the filter paper was removed, the area washed with 0.9% saline and the skin was closed with 4.0 suture. Normal saline filter paper was used in the sham group. The success of the MCAT was checked by hematoxylin-eosin staining of cortical slices. Rats were selected for further hyperlipidemia experiments if their neurological deficit score 24 hours after surgery was ≥ 1 (Karatas et al., 2011).

Electroacupuncture manipulation

One acupoint 2 mm in front of GV20 (GV20 lies in the middle of parietal bone) was selected to connect with EA. ST40 lies in middle fibula, about 7 mm below fibula capitulum. Disposable sterile needles (0.3 mm × 25.0 mm; Beijing Zhongyan Taihe Medical Devices Co., Ltd., Beijing, China) were used to stimulate bilateral ST40 with depth 7 mm, GV20 and the acupoint 2 mm in front of GV20 with depth of 2 mm, and the needling angle was 30°. They were connected respectively with Han's acupoint nerve stimulator (LH202H, Beijing Huawei Industrial Development Company, Beijing, China). Sparse-dense wave stimulation with an alternating frequency of 2/100 Hz was used, with an intensity of 1–2–3 mA (Zhan et al., 2018). The stimulation was continued for 20 minutes once a day.

Behavioral analysis

Rats were scored for their neurological function at 24 hours after surgery with the modified Bederson 5-point neurological deficit score (Longa et al., 1989).

The scoring criteria are as follows: score 0, rat showed complete normality and no neurological deficits (normal); score 1, contralateral front paw cannot be stretched when lifted the tail (mild); score 2, rat circled to the contralateral side (moderate); score 3, rats lean to contralateral side (severe); score 4, rat cannot move autonomously, lost consciousness (extremely severe). Those with neurological deficit score ≥ 1 were selected as successful model.

Tissue preparation

Five rats from each group were selected. Samples of blood

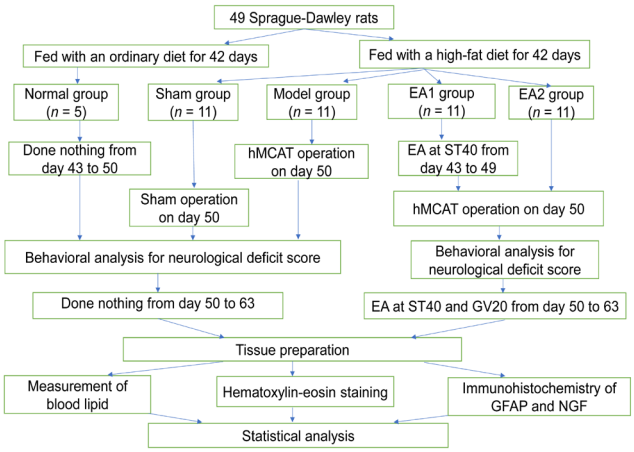

Figure 1 | **Experimental flow chart.**
EA: Electroacupuncture; EA1: electroacupuncture group 1; EA2: electroacupuncture group 2; GFAP: glial fibrillary acidic protein; GV20: the acupoint *Baihui*; hMCAT: hyperlipidemia and middle cerebral artery thrombus; NGF: nerve growth factor; ST40: the acupoint *Fenglong*.

(2 mL) were taken from the orbital vein, at days 1 and 7, and from the abdominal aorta at day 14 after the operation, under anesthesia with 10% pentobarbital sodium, 40 mg/kg, intraperitoneally. The rats were sacrificed with an overdose of pentobarbital sodium on day 14. Blood samples were separated by centrifugation (ST16R, Thermo Fisher Scientific, Waltham, MA, USA) at 3500 r/min for 20 minutes at 4°C, and the serum was stored at –80°C.

Two rats from the normal group were sacrificed and two rats from each experimental group were sacrificed at 1, 7 and 14 days after the MCAT or sham operation. Each rat was injected with 10% pentobarbital sodium and sacrificed with an overdose of anesthetic. The perfusion needle was inserted into the ascending aorta and clamped by forceps. After cutting the right atrial appendage, 300 mL cold saline was perfused until the color of the liver became white. Then, 300–500 mL cold 4% paraformaldehyde was perfused until the limbs were stiff. Each brain was fixed for 48 hours in 4% paraformaldehyde prior to immunostaining.

They were dehydrated in graded ethanol series, cleared in xylene and embedded in paraffin wax. Sections of 5 μm thickness were cut using a microtome (LEITZ-1516, Leica, Solms, Germany).

Measurement of blood lipid
Blood lipids: total cholesterol (TC), triglyceride (TG), low-density lipoprotein (LDL) and high-density lipoprotein (HDL) were measured by Dongzhimen Hospital, Beijing University of Chinese Medicine, China. Biochemical method used a biochemical analyzer (Au5800, Beckman Coulter, Inc., Brea, CA, USA).

Hematoxylin-eosin staining
Two slices were selected at 24 hours after surgery. After paraffin sections were dewaxed, hematoxylin-eosin staining was performed. After gradient alcohol dehydration, the slices were cleared with xylene and mounted with neutral resin. The stained slices were observed under a BX40F4 microscope (Olympus Optical Co., Ltd., Tokyo, Japan).

Immunohistochemistry of GFAP and NGF
Two rats from each group were selected at each time point. Six hippocampal slices were selected. Paraffin slices were conventionally dewaxed to water, soaked in distilled water for 5 minutes, and soaked in phosphate-buffered saline (PBS) for 5 minutes × 3. Slices were incubated in 3% H_2O_2 at room temperature for 10 minutes to eliminate endogenous peroxidase activity. After three washes with PBS each for 5 minutes, the slices were put into 0.01 M citrate buffer (pH 6.0) and microwaved for 35 minutes for antigen retrieval. After three washes with PBS each for 5 minutes, the slices were blocked with 5% bovine serum albumin for 30 minutes at 37°C, and incubated in mouse anti-rat GFAP antibody (astrocyte marker, monoclonal antibody; 1:100; Boster Biological Technology Co., Ltd., Wuhan, China) overnight at 4°C. After three washes with PBS each for 5 minutes, the slices were incubated with goat anti-mouse IgG labeled with secondary anti-horseradish peroxide (Boster Biological Technology Co., Ltd.) at 37°C for 30 minutes. After three washes with PBS each for 5 minutes, the slices were visualized in diaminobenzidine chromogenic solution (Boster Biological Technology Co., Ltd.). When yellow particles appeared, the reaction was terminated by adding water. Slices were dehydrated, cleared, and sealed. PBS 0.01 M was used as a negative control instead of a primary antibody. The immunohistochemical procedure of NGF was the same as that of GFAP. Primary antibody was rabbit-anti rat NGF antibody (monoclonal antibody; 1:250; Abcam (Shanghai) Trading Co., Ltd., Shanghai, China). Secondary antibody was goat anti-rabbit IgG (Boster Biological Technology Co., Ltd.).

Three consecutive hippocampal sections were selected from each brain tissue of two rats for each experimental period. The sections were observed with optical microscope (Olympus BX40F4, Olympus Optical Co., Ltd.). Cells in the hippocampal CA1 region were quantified using Image Pro Plus software 5.0 (Media Cybernetics, Silver Spring, USA) to calculate the average optical density (AOD) per high magnification field.

Statistical analysis
Data were analyzed using SPSS 20.0 software (IBM, Armonk, NY, USA). The data of neurological deficit scores were expressed as the median (quartile range) [*Md* (P_{25}, P_{75})] and Kruskal-Wallis *H* with Dunn-Bonferroni *post hoc* test were used to obtain inter-group comparisons. Results, except neurological deficit scores, are expressed as the mean ± standard deviation (SD). The data of blood lipids and GFAP and NGF were analyzed by one-way analysis of variance followed by least significant difference or Dunnett-*t* *post hoc* test for inter-group comparison. Values of $P < 0.05$ were considered statistically significant.

Results
Loss of animal numbers
Of the 57 rats, 2 died from surgical complications in the model group; 3 died during the 7-day recovery period in the EA1 group; 1 died from surgical complications and 2 died during the 14-day recovery period in the EA2 group. The total loss rate was 14% (8/57). A total of 49 rats remained and were grouped as follows: normal group ($n = 5$), sham group ($n = 11$), model group ($n = 11$), EA1 group ($n = 11$), EA2 group ($n = 11$). The flow chart of the study is shown in **Figure 1**.

Effect of EA on blood lipids
Compared with the normal group, total cholesterol (TC) and low-density lipoprotein (LDL) increased significantly ($P < 0.05$) on days 1, 7, and 14 post-operation and high-density lipoprotein (HDL) decreased significantly ($P < 0.05$) on day 7 post-operation in the model group. Compared with the model group, TC decreased significantly in the EA1 group ($P < 0.05$) on day 1 post-operation and in the EA2 group ($P < 0.05$) on days 1 and 14 post-operation. LDL decreased significantly in the EA1 group ($P < 0.05$) on days 7 and 14 post-operation and in the EA2 group ($P < 0.05$) on days 14 post-operation. There was no significant difference between the EA1 and EA2 groups (**Table 1**).

Effect of EA on behavior
Neurological deficit scores were evaluated 24 hours after

Table 1 | **Blood lipids (mM) post-operation**

Groups	Time (d)	TC	TG	HDL	LDL
Normal	1	1.43±0.10	0.61±0.09	0.51±0.06	0.14±0.01
	7	1.41±0.14	0.61±0.12	0.54±0.05	0.15±0.02
	14	1.53±0.19	0.65±0.17	0.55±0.04	0.12±0.01
Sham	1	2.38±0.18*	0.81±0.07	0.45±0.06	0.64±0.15*
	7	1.72±0.07*	1.12±0.56	0.35±0.11*	0.55±0.11*
	14	2.83±0.39*	1.51±0.12*	0.40±0.06*	1.03±0.16*
Model	1	2.23±0.22*	0.82±0.12	0.45±0.06	0.63±0.06*
	7	1.98±0.25*	1.49±0.48	0.38±0.09*	0.55±0.09*
	14	2.29±0.07*	1.40±0.46	0.44±0.10	0.70±0.15$^{*\#}$
EA1	1	2.00±0.07$^{*\#\dagger}$	0.77±0.13	0.46±0.06	0.64±0.08*
	7	1.69±0.25	0.71±0.14	0.52±0.11$^{\#}$	0.39±0.07*†
	14	1.74±0.28$^{\#}$	0.97±0.23$^{\#}$	0.52±0.04	0.45±0.12$^{*\#\dagger}$
EA2	1	2.02±0.13$^{*\#\dagger}$	0.77±0.13	0.46±0.06	0.64±0.06*
	7	1.71±0.33*	0.86±0.26	0.47±0.16	0.36±0.04*
	14	1.82±0.19$^{\#\dagger}$	1.01±0.33	0.50±0.05	0.50±0.08$^{*\#\dagger}$

Data are expressed as the mean ± SD (n = 5; one-way analysis of variance followed by the least significant difference *post hoc* test). *P < 0.05, *vs*. normal group; #P < 0.05, *vs*. sham group; †P < 0.05, *vs*. model group. EA1: Electroacupuncture group 1; EA2: electroacupuncture group 2; HDL: high-density lipoprotein; LDL: low-density lipoprotein; TC: total cholesterol; TG: triglyceride.

Table 2 | **Neurological deficit scores at 24 hours after operation**

Groups	Neurological deficit score
Sham	0(0,0)
Model	2(2,3)$^{\#}$
EA1	1(1,1)$^{\#\dagger}$
EA2	1(1,2)$^{\#}$
H	20.000
P	0.045

Data are expressed as the median [$Md(P_{25}, P_{75})$] (n = 5; Kruskal-Wallis H test). #P < 0.05, *vs*. sham group; †P < 0.05, *vs*. model group. EA1: Electroacupuncture group 1; EA2: electroacupuncture group 2.

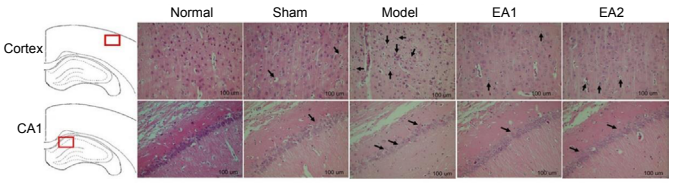

Figure 2 | **Hematoxylin-eosin staining results of ischemic penumbra and hippocampal CA1 region on day 1 post-operation.**
In the cortex, the visual field was the ischemic penumbra beside the ischemic focus. Dyeing with hematoxylin and eosin under the optical microscope at 400× magnification. Scale bars: 100 μm. Arrows indicate cells with large changes in cell morphology. EA: Electroacupuncture.

operation. In model group, rats showed the effects of a poor diet by deficiencies in their behavior. The front paws on the contralateral side could not be extended when rats were lifted by the tail. Some rats circled to contralateral side and a few rats had difficulty in moving. In EA group, rats showed mild deficient behavior. Compared with the sham group, the neurological deficit scores increased significantly in the model group (P < 0.05). Compared with the model group, neurological deficit score decreased significantly in the EA1 group (P < 0.05; **Table 2**).

Changes in cell morphology

Hematoxylin-eosin staining indicated that neurons in the penumbral cortex in the normal group were round, uniform in size and well ordered with well characterized round pale blue nuclei. The morphology of neurons in the sham group was almost normal, with regular arrangement and a clear hierarchy. Nuclei were distinctly visible with no edema. A few neurons had pyknotic nuclei. In the model group, many cells had lost structural integrity. The cellular outline was indistinct and the internal structures were disordered. They were oval or triangular, with dense cytoplasm and pyknotic dark blue nuclei and sparsely arranged. The intercellular space was enlarged and many vacuoles were seen in the cytoplasm. A few nuclei stained red. In all EA groups, the various damaging changes to brain tissue were reduced by varying degrees. Compared with the model group, the quantity and morphology of neurons were significantly better. The morphology of neurons in EA1 was close to normal. There were many intact neurons. Only a few neurons had dark blue pyknotic nucleus. The morphology of neurons indicated that the EA1 group showed more improvement than that of the EA2 group.

Neurons in the hippocampal CA1 region in the normal and sham groups were arranged regularly with clear layers. Neurons in the model group were arranged irregularly with larger intercellular spaces than in the normal group and a few neurons had lost structural integrity. Neurons in the EA groups were similar to those in the normal group (**Figure 2**).

Effect of EA on GFAP and NGF

Immunohistochemical labelling for $GFAP^+$ and NGF^+ showed the cytoplasm was stained brown in cells of the hippocampal CA1 region. In the sham group, the few stained $GFAP^+$ and NGF^+ cells were arranged regularly in the CA1 region. $GFAP^+$ cells had small bodies and slender protrusions stained light brown, indicating a resting state. NGF^+ cells were oval shaped with light brown color. In the model group, numerous $GFAP^+$ and NGF^+ cells were stained dark brown and arranged irregularly. $GFAP^+$ cell bodies had hypertrophied with numerous thicker and longer protrusions, an indication of an activated morphology. In the EA group, $GFAP^+$ and NGF^+ cells were arranged regularly and stained dark brown. $GFAP^+$ cell bodies had shrunk, with shorter protrusions than those in the model group (**Figure 3A** and **C**).

Compared with the normal group, the $GFAP^+$ immunostaining AOD increased significantly on days 1, 7, and 14 post-operation in the model group (P < 0.05). Compared with the sham group, the $GFAP^+$ immunostaining AOD increased significantly on days 1 and 7 post-operation in the model group (P < 0.05) and on day 7 post-operation in the EA2 group (P < 0.05), and decreased significantly on day 14 post-operation in the EA1 group (P < 0.05). Compared with the model group, the GFAP AOD decreased significantly on days 1, 7, and 14 post-operation in the EA1 group (P < 0.05) and decreased significantly on day 1 post-operation in the EA2 group (P < 0.05). Compared with the EA1 group, the GFAP AOD had not changed much on days 1 and 7, but was significantly higher on day 14 post-operation in the EA2 group (P < 0.05; **Figure 3B**).

Compared with the normal group, the NGF AOD increased significantly (P < 0.05) on days 7 and 14 post-operation in the model group. Compared with the sham group, the NGF AOD increased on days 7 and 14 post-operation in the model group (P < 0.05) and on days 7 and 14 post-operation (P < 0.05) in both EA groups. Compared with the model group, the NGF AOD increased on days 7 and 14 post-operation in the EA1 group (P < 0.05; **Figure 3D**).

Discussion

Hyperlipidemia patients always have high TC, TG, and LDL levels and low HDL levels in their serum. Abnormalities of TC, TG, and LDL can trigger inflammation and eventually lead to atherosclerosis, which is a common cause of ischemic stroke (Wang et al., 2018). It has been shown that rates of cardiovascular events decrease following cholesterol reduction treatment in patients with hyperlipidemias (Ridker, 2014).

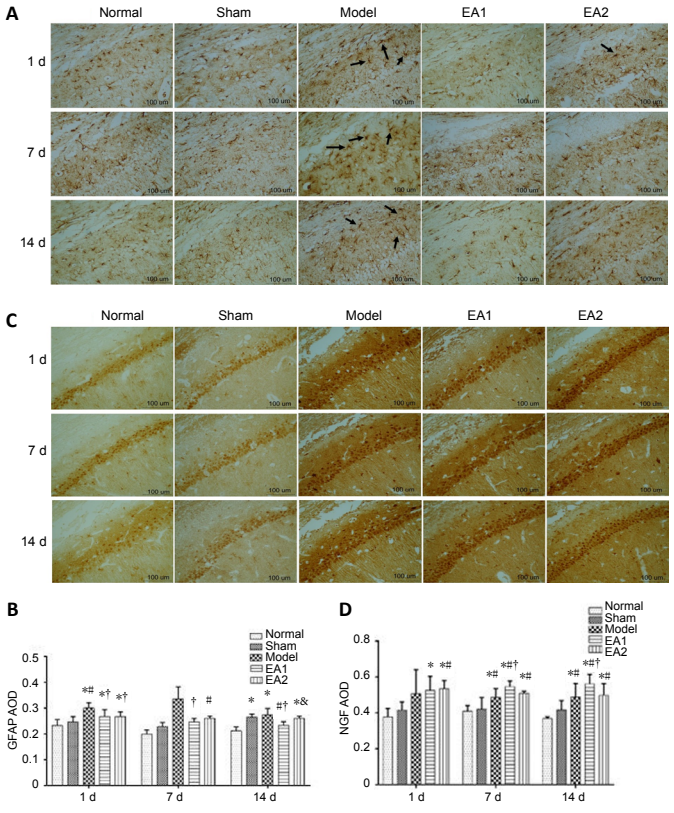

Figure 3 | **Immunohistochemical results of GFAP and NGF in the hippocampal CA1 region on days 1, 7 and 14 post-operation.**
The abscissa of B and D is time grouping. Cells with brown protrusions are GFAP-positive cells; and cells with brown granules in cytoplasm are NGF-positive cells. (A, C) Immunohistochemical figures of GFAP and NGF in the hippocampal CA1 region. Arrows indicate reactive astrocytes. Dyeing with immunohistochemical method under the optical microscope (original magnification, 400×). Scale bars: 100 μm. (B, D) Histogram results of GFAP and NGF AOD. Data are expressed as the mean ± SD (n = 6 slices), one-way analysis of variance followed by Dunnett-*t post hoc* test. *P < 0.05, *vs*. normal group; #P < 0.05, *vs*. sham group; †P < 0.05, *vs*. model group; &P < 0.05, *vs*. EA1 group. AOD: Average optical density; EA: electroacupuncture; GFAP: glial fibrillary acidic protein; NGF: nerve growth factor.

We found that high-fat diet feeding for 7 weeks can increase TC, TG, and LDL in hMCAT rats at serum level, and EA can reduce TC and LDL levels. It was shown that EA was effective in regulating blood lipid. However, we did not find any difference between the two EA methods; the reason may be that the acupuncture pre-stimulation intervention time was short.

Hyperlipidemia can destroy the balance of neurotransmitters in the brain (Valladolid et al., 2012; Sandoval-Salazar et al., 2016), destroy the structure of hippocampal neurons, and damage cerebral vessels and neurons. Some studies have found that hyperlipidemia may activate astrocytes through high levels of TG, TC and LDL and has direct toxic effects on cerebral vessels and neurons in the rat brain (Yang et al., 2017). Other studies have explored the relationship between NGF and blood lipids as an explanation of the clinical risk factors of cerebral ischemia. Some found that TC and TG were negatively correlated with NGF (Atanassova et al., 2014; Dan et al., 2019). Others found that NGF increased the absorption of LDL and thereby play a metabolic and morphological role in neurons (Do et al., 2016). Other research largely confirms that hyperlipidemia enhances brain injury following ischemic stroke by processes of oxidative stress, inflammation, and apoptosis of nerve cells (Cao et al., 2015). Our research combines hyperlipidemia and cerebral ischemia in a model that mimics that in clinical practice. It explores the mechanism of EA in reducing blood lipid, improving stroke behavior and repairing brain injury from the perspective of neural stem cell repair. Therefore, this experiment focused on investigating the changes in astrocytes and NGF following hyperlipidemia-cerebral ischemia and explores the mechanism of EA action in treating stroke.

Astrocytes are the most numerous cells in the brain in the central nervous system and play critical roles in the physiology of the central nervous system (Filous et al., 2016). GFAP, an intermediate filament protein, is expressed in astrocytes in the central nervous system (Hol et al., 2015). GFAP is traditionally a specific marker for astrocytes immunoreaction and its increase is generally accepted as a sign of pathological astroglial response. Under pathological conditions such as cerebral ischemia, astrocytes changed rapidly to their reactive state. Activation of astrocytes causes the production and release of various pro-inflammatory cytokines and chemokines, which eventually leads to the formation of an astroglial scar (Shang et al., 2019). On the one hand, activated astrocytes can enhance the ability of RAS in absorbing and transforming Glutamic after ischemia, which reduces the accumulation of extracellular Glutamic, thus reducing secondary neurotoxicity caused by excitatory amino acids (Chen et al., 2003). Simultaneously, they release NGF, enhance neuronal survival and reduce local inflammation (Sofroniew, 2005). On the other hand, reactive astrocytes also secrete factors that contribute to cell death, including glutamate and the pro-inflammatory cytokine tumor necrosis factor (Swanson et al., 2004; Sofroniew, 2009). Besides their toxic effects, these factors may be abnormally involved metaplasticity mechanism and inhibit long-term potentiation (Jones, 2015). It has been shown that EA can inhibit GFAP expression triggered by cerebral ischemia, reduce inflammation and promote the proliferation of nerve cells, thus reducing brain injury (Jia et al., 2017; Kim et al., 2018). In this study, GFAP in the hippocampal CA1 region of astrocytes was upregulated 24 hours after hMCAT and maintained for the 14 days of the experiment, and the peak was at 7 days. The upregulated trend is consistent with the previous study.

NGF can promote synaptic growth, nourish neurons, regulate the growth, development, and differentiation of neurons in the central nervous system, playing a neuroprotective effect on brain tissue (Ziv-Polat et al., 2014). Cerebral ischemia can upregulate NGF protein expression in the ipsilateral cortex and hippocampus, which may be an endogenous protective mechanism for maintaining neuronal survival in injury areas of the brain (Liu et al., 2018). Astrocytes have a close relationship with nerve growth factor. On the one hand, astrocytes secrete a variety of neurotrophic factors, including NGF, to support neuronal survival and promote synaptic growth. On the other hand, NGF can promote astrocyte differentiation, nerve repair and regeneration (Davis et al., 2018). In this study, NGF in the hippocampal CA1 region was upregulated 24 hours after hMCAT, maintained for 14 days, and peaked at 1 day.

Compared with thrombolysis therapy, acupuncture is a safer and cheaper treatment for hyperlipidemia and stroke. Our data suggest that both EA prescriptions can inhibit the excessive production of GFAP and improve NGF secretion.

The limitations of this study are as follows: the number of animals was small at each time point. The relationship between astrocytes and NGF needs further investigations. The difference between EA1 and EA2 is not obvious. In the future, we hope to retest the theory using a larger sample number and prolonging the acupuncture intervention time to explore the signaling pathway between GFAP and NGF.

The results showed that EA can adjust blood lipid metabolism, inhibit astrocyte changes and promote NGF secretion in the hippocampal CA1 region after hyperlipidemia with cerebral ischemia. EA at ST40 after the establishment of hyperlipidemia and at GV20 and ST40 after combined hyperlipidemia with cerebral ischemia has stronger effect than EA at GV20 and ST40 after hyperlipidemia with cerebral ischemia.

Author contributions: *Fundraising: XJR; study design: XJR and YT; study performance: NYX; data analysis and paper writing: NYX; immunohistochemistry experiment: DYG and RJD; manuscript modification: HHK and XJR. All authors read and approved the final manuscript.*
Conflicts of interest: *The authors declare that there are no conflicts of interest associated with this manuscript.*
Financial support: *This study was funded by the National Natural Science Foundation of China, No. 81470200 (to XJR). The funding source had no role in study conception and design, data analysis or interpretation, paper writing or deciding to submit this paper for publication.*
Institutional review board statement: *All experimental procedures and protocols were approved by the Animal Use and Management Committee of Beijing University of Chinese Medicine, China (approval No. BUCM-3-2018022802-1002) on April 12, 2018.*

Data sharing statement: Datasets analyzed during the current study are available from the corresponding author on reasonable request.
Plagiarism check: *Checked twice by iThenticate.*
Peer review: *Externally peer reviewed.*

Open peer reviewer: *Melanie G. Urbanchek, University of Michigan, USA.*
Additional file: *Open peer review report 1.*

References

Atanassova P, Hrischev P, Orbetzova M, Nikolov P, Nikolova J, Georgieva E (2014) Expression of leptin, NGF and adiponectin in metabolic syndrome. Folia Biol (Krakow) 62:301-306.

Baldivia DDS, Sanjinez-Argandoñ EJ, Antunes KÁ, Moraes ICF, Dos Santos EL, de Picoli Souza K (2018) The chemical composition and metabolic effects of attalea phalerata nut oil in hyperlipidemic rats induced by a high-fructose diet. Molecules 23:E960.

Bani-Yaghoub M, Underhill TM, Naus CC (1999) Gap junction blockage interferes with neuronal and astroglial differentiation of mouse P19 embryonal carcinoma cells. Dev Genet 24:69-81.

Cao XL, Du J, Zhang Y, Yan JT, Hu XM (2015) Hyperlipidemia exacerbates cerebral injury through oxidative stress, inflammation and neuronal apoptosis in MCAO/reperfusion rats. Exp Brain Res 233:2753-2765.

Chen Y, Swanson RA (2003) Astrocytes and brain injury. J Cereb Blood Flow Metab 23:137-149.

Davis JB, Calvert V, Roberts S, Bracero S, Petricoin E, Couch R (2018) Induction of nerve growth factor by phorbol 12-myristate 13-acetate is dependent upon the mitogen activated protein kinase pathway. Heliyon 4:e00617.

Do HT, Bruelle C, Pham DD, Jauhiainen M, Eriksson O, Korhonen LT, Lindholm D (2016) Nerve growth factor (NGF) and pro-NGF increase low-density lipoprotein (LDL) receptors in neuronal cells partly by different mechanisms: role of LDL in neurite outgrowth. J Neurochem 136:306-315.

Filous AR, Silver J (2016) Targeting astrocytes in CNS injury and disease: a translational research approach. Prog Neurobiol 144:173-187.

Han X, Chen M, Wang F, Windrem M, Wang S, Shanz S, Xu Q, Oberheim NA, Bekar L, Betstadt S, Silva AJ, Takano T, Goldman SA, Nedergaard M (2013) Forebrain engraftment by human glial progenitor cells enhances synaptic plasticity and learning in adult mice. Cell Stem Cell 12:342-353.

Hol EM, Pekny M (2015) Glial fibrillary acidic protein (GFAP) and the astrocyte intermediate filament system in diseases of the central nervous system. Curr Opin Cell Biol 32:121-130.

Huang J, You XF, Liu WL, Song CM, Lin XM, Zhang XF, Tao J, Chen LD (2017) Electroacupuncture ameliorating post-stroke cognitive impairments via inhibition of peri-infarct astroglial and microglial/macrophage P2 purinoceptors-mediated neuroinflammation and hyperplasia. BMC Complement Altern Med 17:480.

Jones OD (2015) Astrocyte-mediated metaplasticity in the hippocampus: Help or hindrance? Neuroscience 309:113-124.

Karatas H, Erdener SE, Gursoy-Ozdemir Y, Gurer G, Soylemezoglu F, Dunn AK, Dalkara T (2011) Thrombotic distal middle cerebral artery occlusion produced by topical FeCl(3) application: a novel model suitable for intravital microscopy and thrombolysis studies. J Cereb Blood Flow Metab 31:1452-1460.

Kim H, Koo YS, Shin MJ, Kim SY, Shin YB, Choi BT, Yun YJ, Lee SY, Shin HK (2018) Combination of constraint-induced movement therapy with electroacupuncture improves functional recovery following neonatal hypoxic-ischemic brain injury in rats. BioMed Res Int doi: 10.1155 / 2018/8638294.

Kim H, Park JH, Shin MC, Cho JH, Lee TK, Kim H, Song M, Park CW, Park YE, Lee JC, Ryoo S, Kim YM, Kim DW, Hwang IK, Choi SY, Won MH, Ahn JH (2019) Fate of astrocytes in the gerbil hippocampus after transient global cerebral ischemia. Int J Mol Sci 20:845.

Li J, Ma N, Chen J, Yan D, Zhang Q, Shi J (2019) EphA4 receptor regulates outwardly rectifying chloride channel in CA1 hippocampal neurons after ischemia-reperfusion. Neuroreport 30:980-984.

Liu H, Zhong LL, Zhang YW, Liu XW, Li J (2018) Rutin attenuates cerebral ischemia/reperfusion injury in ovariectomized rats via estrogen receptor-mediated BDNF-TrkB and NGF-TrkA signaling. Biochem Cell Biol 96:1-35.

Longa EZ, Weinstein PR, Carlson S, Cummins R (1989) Reversible middle cerebral artery occlusion without craniectomy in rats. Stroke 20:84-91.

Mao JR, Ge DY, Dong RJ, Zhao LY, Li GM, Ren XJ (2018) Effects of electroacupuncture on astrocytes at subventricular zone in rats with hyperlipidemia and cerebral ischemia. J Beijing Univ TCM 41:1025-1032, 1040.

National Research Council (2011) NIH Guide for the Care and Use of Laboratory Animals. 8th ed. Washington DC: the National Academies Press.

O'Keeffe GW, Gutierrez H, Howard L, Laurie CW, Osorio C, Gavalda N, Wyatt SL, Davies AM (2016) Region-specific role of growth differentiation factor-5 in the establishment of sympathetic innervation. Neural Dev 11:4.

Ouyang YB, Xu L, Yue S, Liu S, Giffard RG (2014) Neuroprotection by astrocytes in brain ischemia: importance of microRNAs. Neurosci Lett 565:53-58.

Pham DD, Bruelle C, Thi Do H, Pajanoja C, Jin C, Srinivasan V, Olkkonen VM, Eriksson O, Jauhiainen M, Lalowski M, Lindholm D (2019) Caspase-2 and p75 neurotrophin receptor (p75NTR) are involed in the regulation of SREBP and lipid genes in hepatocyte cells. Cell Death Dis 10:537.

Ridker PM (2014) LDL cholesterol: controversies and future therapeutic directions. Lancet 384:607-617.

Sandoval-Salazar C, Ramirez-Emiliano J, Trejo-Bahena A, Oviedo-Solis CI, Solis-Ortiz MS (2016) A high-fat diet decreases GABA concentration in the frontal cortex and hippocampus of rats. Biol Res 49:15-20.

Shang S, Liu L, Wu X, Fan F, Hu E, Wang L, Ding Y, Zhang Y, Lu X (2019) Inhibition of PI3Kgamma by AS605240 protects tMCAO mice by attenuating pro-inflammatory signaling and cytokine release in reactive astrocytes. Neuroscience 415:107-120.

Sofroniew MV (2005) Reactive astrocytes in neural repair and protection. Neuroscientist 11:400-407.

Sofroniew MV (2009) Molecular dissection of reactive astrogliosis and glial scar formation. Trends Neurosci 32:638-647.

Swanson RA, Ying W, Kauppinen TM (2004) Astrocyte influences on ischemic neuronal death. Curr Mol Med 4:193-205.

Trendelenburg G, Dirnagl U (2005) Neuroprotective role of astrocytes in cerebral ischemia: focus on ischemic preconditioning. Glia 50:307-320.

Valladolid-Acebes I, Merino B, Principato A, Fole A, Barbas C, Lorenzo MP (2012) High-fat diets induce changes in hippocampal glutamate metabolism and neurotransmission. Am J Physiol Endocrinol Metab 302:E396-402.

Wang LD, Liu JM, Yang Y, Peng B, Wang YL (2019) The prevention and treatment of stroke still face huge challenges-brief report on stroke prevention and treatment in China, 2018. Zhongguo Xunhuan Zazhi 34:105-119.

Wang LL, He ML, Zhang Y (2018) Risk factors associated with extracranial atherosclerosis in old patients with acute ischemic stroke. Sci Rep 8:12541.

Yang N, Song Y, Dong B, Li Y, Kou L, Yang J, Qin Q (2018) Elevated interleukin-38 level associates with clinical response to atorvastatin in patients with hyperlipidemia. Cell Physiol Biochem 49:653-661.

Yang W, Shi H, Zhang J, Shen Z, Zhou G, Hu M (2017) Effects of the duration of hyperlipidemia on cerebral lipids, vessels and neurons in rats. Lipids Health Dis 16:26-34.

Zhan J, Pan R, Zhou M, Tan F, Huang Z, Dong J, Wen Z (2018) Electroacupuncture as an adjunctive therapy for motor dysfunction in acute stroke survivors: a systematic review and meta-analyses. BMJ Open 8:e017153.

Ziv-Polat O, Shahar A, Levy I, Skaat H, Neuman S, Fregnan F, Geuna S, Grothe C, Haastert-Talini K, Margel S (2014) The role of neurotrophic factors conjugated to iron oxide nanoparticles in peripheral nerve regeneration: in vitro studies. Biomed Res Int 2014:267808.

P-Reviewer: Urbanchek MG; C-Editor: Zhao M; S-Editors: Wang J, Li CH; L-Editors: Dawes EA, Yajima W, Qiu Y, Song LP; T-Editor: Jia Y